22nd IAHR International Symposium on Ice
Singapore, August 11 to 15, 2014

Modelling ice ridge punch tests with cohesive 3D discrete element method

Arto Sorsimo, Jaakko Heinonen
VTT Technical Research Centre of Finland
Kemistintie 3,02044 Espoo
arto.sorsimo@vtt.fi, jaakko.heinonen@vtt.fi

In this paper we simulate a punch through test of partly consolidated ice ridge keel with three dimensional discrete element method. We model the contact forces between discrete ice blocks with Hertz-Mindlin contact model. For freeze bonds between the ice blocks we apply classical linear cohesion model with few modifications. In simulations we vary the parameters that are most relevant to maximum force on indenter and examine the causalities due to variation. In addition, the failure mechanisms in ice rubble are studied. We compare the simulation results to full-scale experimental results to confirm the feasibility of the model. The results show that the simulations are in excellent agreement with the previous results. Based on simulations, we are able to determine the main characteristics of an ice ridge from material parameters of ice and freeze bonds. Furthermore, we conclude that the model introduced can be used in other applications within ice mechanics.

1. Introduction

The world around us changes constantly. During last ten years, more attention has been brought to global warming. According to latest forecasts, the Arctic will be almost completely ice-free in 2050, latest (Overland & Wang, 2013). This poses major threat to the Arctic wildlife, but on the other hand opens new possibilities for drilling and shipping in the region.

However, great new possibilities come with great new challenges. One of the major challenges is the integrity of man-made structures in arctic climates. Ice ridges are typical features in cold environments that are formed when large ice floes collide to each other and broken ice blocks pile up under and above the ice floe and eventually freeze together. The part below the water surface ranges typically between 5 to 30 meters (Leppäranta, 2011), which can cause severe damage to structures such as wind turbines, oil rigs, ships etc.

There are essentially two different ways to calculate ice ridge loads on a structure – analytical and numerical. Analytical approach relies on data obtained from experimental investigations. However, even though several articles on experiments with model scale have been presented, only few full-scale experiments have been conducted.

In numerical simulations ice ridges have been modeled mainly with finite element method which assumes that the keel is a continuous. This approach provides a solid base for approximating maximum loads on a structure (Heinonen, 2004), but the adaptability of the model decreases if the number of discrete ice blocks is small compared to the size of the ice ridge. One suitable candidate to model such discontinuous medium is discrete element method.

Discrete element method (DEM) is a method that computes the motion of large number of distinct particles, Contact forces between rigid particles are calculated with specific contact models. One of the first usages of DEM within ice mechanics was the examination of ice ridging (Hopkins, 1992), (Hopkins, et al., 1999). Lately it has also been applied to other subfields, e.g. ice floes interaction with off-shore structures (Paavilainen & Tuhkuri, January 2013), wet-snow avalanches (Favier, et al., 2013) and ice rubble (Polojärvi & Tuhkuri, 2009), (Polojärvi & Tuhkuri, 2013). For further development of the DEM regarding ice rubble, another paper in IAHR 2014, written by Polojärvi and Tuhkuri (2014) introduced an expansion from 2D to 3D where ice ridge punch tests were modelled with polyhedral ice blocks and freeze bonds.

2. Theory and methods

All the particles in the simulation are subjected to gravity and buoyancy of water. In addition to the field forces, we model the interaction forces between the particles with a contact model that comprises of two parts; Hertz-Mindlin contact model and cohesive freeze bond.

Hertz-Mindlin contact model describes elastic contacts between ice particles and geometries, while the improved cohesive freeze bond model's objective is to grasp a sense of reality for freeze bonds between ice blocks.

Total force acting on each particle is determined on every time step of simulation by summing up all the contact forces. The set of equations for contact forces that are calculated on every time step is

$$
\begin{aligned}
\sum \boldsymbol{F}_n &= \boldsymbol{F}_{H,n} + \boldsymbol{F}_{HD,n} + \boldsymbol{F}_{B,n} \\
\sum \boldsymbol{F}_t &= \boldsymbol{F}_{H,t} + \boldsymbol{F}_{C,t} + \boldsymbol{F}_{HD,t} + \boldsymbol{F}_{B,t} \\
\sum \boldsymbol{M}_n &= \boldsymbol{M}_{rf} + \boldsymbol{M}_{B,n} \\
\sum \boldsymbol{M}_t &= \boldsymbol{M}_{rf} + \boldsymbol{M}_{B,t}
\end{aligned}
\qquad \textbf{[1]}
$$

where $\boldsymbol{F}_{H,n} \in \mathbb{R}^3$ and $\boldsymbol{F}_{H,t} \in \mathbb{R}^3$ are the Hertzian normal and tangential force, respectively, $\boldsymbol{F}_{\mathrm{C},i} \in \mathbb{R}^3$ is the Coulomb friction force, $\boldsymbol{M}_{rf,i} \in \mathbb{R}^3$ is the rolling friction torque from equation, $\boldsymbol{F}_{HD,n} \in \mathbb{R}^3$ and $\boldsymbol{F}_{HD,t} \in \mathbb{R}^3$ are the damping force in the normal and tangential direction, respectively, $\boldsymbol{F}_{B,n} \in \mathbb{R}^3$ and $\boldsymbol{F}_{B,t} \in \mathbb{R}^3$ are the normal and tangential force for the freeze bond, $\boldsymbol{M}_{B,n} \in \mathbb{R}^3$ and $\boldsymbol{M}_{B,t} \in \mathbb{R}^3$ are the normal and tangential moment for the freeze bond.

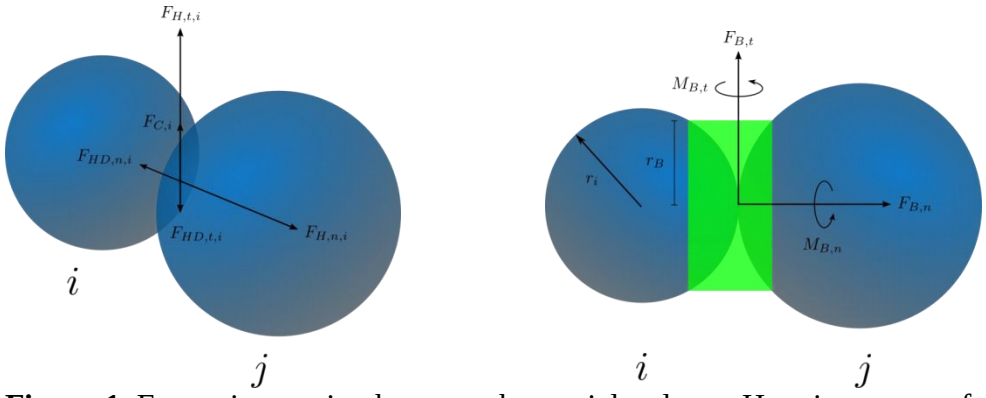

Figure 1. Forces interacting between the particles due to Hertzian contact forces (left) and freeze bond forces (right).

We calculate the magnitude of the effective stress from

$$
\sigma_* = \sqrt{\left|\boldsymbol{\sigma}\right|^2 + \beta^{-2}\left|\boldsymbol{\tau}\right|^2}\,, \qquad \textbf{[2]}
$$

where $\beta \in \mathbb{R}_+$ is the shear stress factor and the normal stress $\boldsymbol{\sigma} \in \mathbb{R}^3$ and shear stress $\boldsymbol{\tau} \in \mathbb{R}^3$ are defined as

$$
\boldsymbol{\sigma} = \frac{\boldsymbol{F}_{B,n}}{A_B} + \frac{\boldsymbol{M}_{B,t}}{J_{tt}} r_B \qquad \textbf{[3]}
$$

$$
\boldsymbol{\tau} = \frac{\boldsymbol{F}_{B,t}}{A_B} + \frac{\boldsymbol{M}_{B,n}}{J_{nn}} r_B\,, \qquad \textbf{[4]}
$$

where $r_B \in \mathbb{R}$ is the bond radius, $\pi r_B^2 = A_B \in \mathbb{R}$ is the bond area, $\frac{1}{2}\pi r_B^4 = 2 \cdot J_{tt} = J_{nn} \in \mathbb{R}$ is the second normal and tangential moment of area, respectively. Correspondingly we calculate the magnitude of the effective separation from

$$\delta_* = \sqrt{\left|\boldsymbol{\chi}_n + r_B \boldsymbol{\theta}_t\right|^2 + \left|\boldsymbol{\chi}_t + r_B \boldsymbol{\theta}_n\right|^2}\,, \qquad \textbf{[5]}$$

where $\boldsymbol{\chi}_n \in \mathbb{R}^3$ and $\boldsymbol{\chi}_t \in \mathbb{R}^3$ are the relative normal and tangential separation vectors, $\boldsymbol{\theta}_n \in \mathbb{R}^3$ and $\boldsymbol{\theta}_t \in \mathbb{R}^3$ are the relative normal and tangential angle.

If the effective stress exceeds the predefined critical stress value, that is $\sigma_* \geq \sigma_{*,cr} \in \mathbb{R}$, dissipative crack growth process is initiated as the freeze bond strength is exceeded. The cohesion model for breakage is a simple linear model with un- and reloading features, cf. (Hillerborg, et al., 1976). For further details of derivation of the model, cf. (Sorsimo & Heinonen, 2014).

We apply the presented model to the numerical simulations, which are benchmarked against the in-situ punch through test #0/2000 conducted by Heinonen (Heinonen, 2004). The purpose of a punch through test is to examine the properties of an ice ridge by pressing the ice rubble downwards with an indenter that produces distinct force graphs. Main emphasis in the simulations is the analysis of ice rubble failure processes and the effects of freeze bond properties to the punch-through test results. In practice, we set all the other parameters fixed in the simulations except the freeze bond parameters under investigation, which we will vary between pre-specified intervals defined in Table 1.

Table 1. Parameters for the simulation.

Type	Parameter	Symbol	Unit	Value	Source
General	Gravity	g	m/s^2	9.81	-
	Water density	ρ_w	kg/m^3	1028	(Leppäranta, 2011)
Ice	Ice density	ρ_i	kg/m^3	920	(Timco & Weeks, 2010)
	Poisson's ratio	ν	-	0.35	(Timco & Weeks, 2010)
	Elastic modulus	E	GPa	2.7	(Timco & Weeks, 2010)
	Shear modulus	G	GPa	$G = E(2(1+\nu))^{-1}$	derived
	Coef. of Restitution	C_r	-	0.8	(Higa, et al., 1998)
	Coef. of Static Friction	μ_s	-	0.5	(Timco & Weeks, 2010)
	Coef. of Rolling Friction	μ_{rf}	-	0.001	approx.
Geometry	Cylinder radius	-	m	10	-
	Indenter diameter	d_{ind}	m	3	(Heinonen, 2004)
	Indenter velocity	-	m/s	0.03	
	Effective keel thickness	h	m	4.6	(Heinonen, 2004)
	Consolidated layer thickness	-	m	0.85	(Heinonen, 2004)
	Ice block radius	r	m	$[0.2275, 0.4725]$	approx.
Freeze bond	Elastic stiffness (bond)	$S_{B,n}$	N/m^3	$[1 \cdot 10^3, 1 \cdot 10^9]$	variable
	Shear stiffness (bond)	$S_{B,t}$	N/m^3	$S_{B,t} = \beta \cdot S_{B,n}$	derived
	Shear stress factor	β	-	$[0, 5]$	variable

Effective strength (part.-part.)	$\sigma_{*,cr,p-p}$	Pa	$[1 \cdot 10^3, 1 \cdot 10^9]$	variable
Effective strength (part.-geom.)	$\sigma_{*,cr,p-g}$	Pa	$\sigma_{*,cr,p-g} = 2 \cdot \sigma_{*,cr,p-p}$	derived
Bond disk scale	BDS	-	$[0.1, 1]$	variable
Bond radius	r_B	m	$U \sim [0.02275, 0.4725]$	derived
Dissipation distance	$\delta_{*,diss}$	μm	20	(Mulmule & Dempsey, 1999)

Simulations and analysis were conducted using EDEM® 2.5.1 particle simulation software, where the freeze bond model with linear cohesion was implemented through API.

3. Results and analysis

The numerical results are in agreement with the experimental results presented in (Heinonen, 2004). In the experiment #0/2000 that we simulated the maximum force was 792 kN, which suits very well into the simulation results. By comparing the simulation data with different parameter values, one can formulate an estimate what were the ice conditions at the time of experiment.

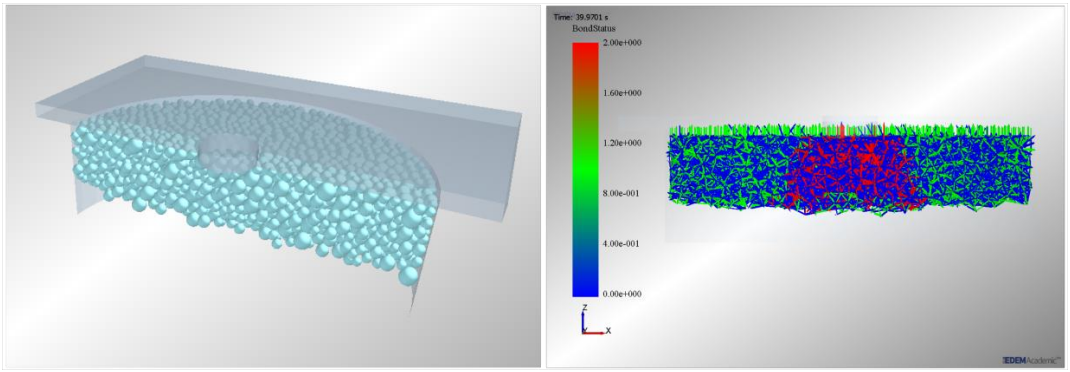

Figure 2. Visual examination of freeze bond breaking process by contact vectors, where green and red colour indicates healthy and broken freeze bond, respectively.

During the simulations three distinct force graphs were noticed that illustrate different breaking patterns that can be classified as continuous, critical and minimal breakage. Typical force graphs on these three situations are illustrated in Figure 3.

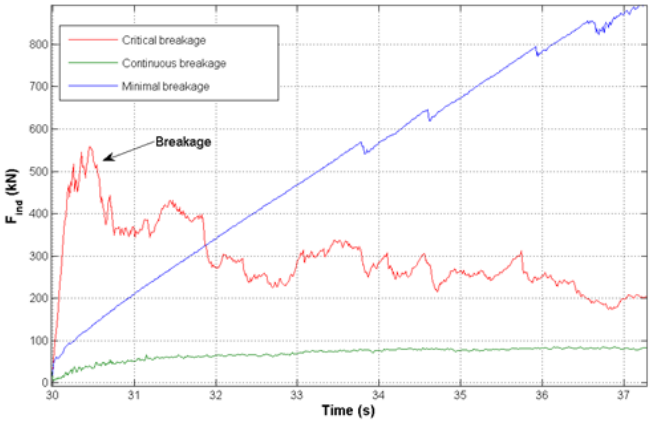

Figure 3. Different types of force diagrams.

In continuous breakage the freeze bonds break continuously as the indenter progresses down. In this case the resistance due to freeze bonds is negligible as the force is almost equivalent to the maximum force on indenter without any freeze bonds. Thus the force on indenter is equal to ice blocks buoyancy force directed upwards.

The case of minimal breakage is the complete opposite to the continuous breakage as most of the freeze bonds do not break at all. As the indenter is displacement driven in the simulations, the maximum force on indenter increases quasilinearly and no sudden breakage occurs.

In the critical breakage the force subjected to freeze bonds increases until the critical value is exceeded and large amount of freeze bond break nearly simultaneously. Hence we note a sudden drop in force diagram, which was the most common failure at late phase found in experiments (Heinonen, 2004). At this point typical cone breaking structure is formed, cf. Figure 2, and the maximum force on indenter during the simulation is achieved.

In the simulations we varied three constitutive parameters for freeze bonds; stiffness, strength and surface area of the freeze bond. The results of the simulations are shown in Figure 4.

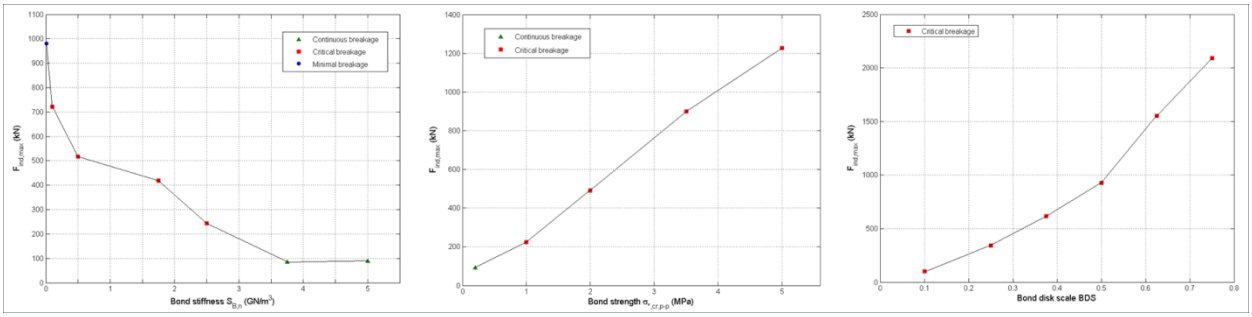

Figure 4. Maximum indenter force as a function of the bond stiffness, bond strength and freeze bond surface area.

We notice that as the freeze bond stiffness increases, the maximum force decreases. With high bond stiffness the bonds are more rigid and thus exert higher force with small displacements. Therefore the bonds break effortlessly and the maximum force on indenter is relatively small. In the opposite case, i.e. low bond stiffness, the ice keel acts analogously to a uniform elastic material as only few bonds break. With reasonable freeze bond stiffness values we achieve a force diagram with critical breakage.

Varying the bond strength leads to opposite results – increasing bond strength increases the maximum force on indenter linearly. This is reasonable since with higher bond strengths more force is required from the indenter to break the ice keel. Note that even with high bond strengths critical breakage is achieved as the indenter is displacement-driven.

Next we examine the bond disk scale, which determines the radius of the freeze bond which will be used to calculate the effective surface area of the freeze bond. Thus by decreasing the bond disk scale can be considered the same as decreasing the effective surface area of freeze bond. The effect of freeze bond surface area is similar to bond strength – increasing surface area

increases the maximum force on indenter. The effect is reasonable as doubling the bond disk scale quadruples the bond force with the same displacement. Since the bond disk scale defines the bond radius of the freeze bond, it can be interpreted as a parameter of how consolidated the ice keel is.

4. Discussion and conclusions

According to the obtained results, we conclude that the Hertz-Mindlin model with linear cohesion is a reasonable model for ice rubble. However, as the exact properties of ice rubble are unknown, more research is required both in experimental and theoretical field of ice rubble mechanics.

It is trivial that the ice blocks within the ice ridge are not spherical particles, but according to results the representation of ice blocks as spheres was sufficient. However, using spherical particles may conceal some aspects of ice ridge that we are not aware but it is nevertheless excellent starting point for a freeze bond model.

The simulation results provide information how the properties of freeze bond affect the results of punch through test. Thus the simulation results can be used to approximate the freeze bonds properties within an ice ridge when experimental data is available. Furthermore, the results provide some information how an ice ridge will behave as it collides with an off-shore structure. More accurate interaction model can be obtained by using the presented model and running a simulation where an ice ridge interacts with rigid structure. This will be left as future work.

Acknowledgments

We would like to show our gratitude to the financiers of this project, Tekes - the Finnish Funding Agency for Technology and Innovation, Aker Arctic Technology Inc., Fennovoima Ltd and Finnish Transport Safety Agency Trafi. In addition, the authors wish to acknowledge the support from the Research Council of Norway through the Centre for Research-based Innovation SAMCoT and the support from all SAMCoT partners.

References

Cundall, P. A. & Strack, O. D., 1979. A discrete numerical model for granular assemblies. *Geotechnique,* Volume 29, pp. 47-65.

Favier, L., Daudon, D. & Donzé, F.-V., 2013. Rigid obstacle impacted by a supercritical cohesive granular flow using a 3D discrete element model. *Cold Regions Science and Technology,* Volume 85, pp. 232-241.

Heinonen, J., 2004. *Constitutive Modeling of Ice Rubble in First-Year Ridge Keel.* Espoo: VTT Publications 536.

Higa, M., Arakawa, M. & Maeno, N., 1998. Size Dependence of Restitution Coefficients of Ice in Relation to Collision Strength. *Icarus,* 133(2), pp. 310-320.

Hillerborg, A., Modeer, M. & Petersson, P.-E., 1976. Analysis of crack formation and crack growth in concrete by means of fracture mechanics and finite elements. *Cement and Concrete Research,* 6(6), pp. 773-781.

Hopkins, M. A., 1992. Numerical simulation of Systems of Multitudinous Polygonal Blocks. *Cold Regions Research and Engineering Laboratory, CRREL,* p. 69.

Hopkins, M., Tuhkuri, J. & Lensu, M., 1999. Rafting and ridging of thin ice sheets. *Journal of Geophysical Research: Oceans,* 104(C6), pp. 13605-13613.

Leppäranta, M., 2011. *The drift of sea ice.* Berlin: Springerverlag .

Mulmule, S. & Dempsey, J., 1999. Scale effects on sea ice fracture. *Mechanics of Cohesive-Frictional Materials,* Volume 4, pp. 505-524.

NASA, 2013. *GISS Surface Temperature Analysis.* [Online]
Available at: http://data.giss.nasa.gov/gistemp/graphs_v3/Fig.A2.pdf
[Accessed 15 4 2013].

Overland, J. E. & Wang, M., 2013. When will the summer arctic be nearly sea ice free?. *Geophysical Research Letters.*

Paavilainen, J. & Tuhkuri, J., January 2013. Pressure distributions and force chains during simulated ice rubbling against sloped structures. *Cold Regions Science and Technology,* Volume 85, pp. 157-174.

Palosuo, E., 1974. *The Formation and Structure of Ice Ridges in the Baltic,* Helsinki: University of Helsinki.

Polojärvi, A. & Tuhkuri, J., 2009. 3D discrete numerical modelling of ridge keel punch through tests. *Cold Regions Science and Technology,* 56(1), pp. 18-29.

Polojärvi, A. & Tuhkuri, J., 2013. On modeling cohesive ridge keel punch through tests with a combined finite-discrete element method. *Cold Regions Science and Technology,* Volume 85, pp. 191-205.

Polojärvi, A. & Tuhkuri, J., 2014 (Forthcoming). *3D DEM for Freeze Bonded Ice Rubble Consisting of Polyhedral Blocks.* Singapore, 22nd IAHR International Symposium on Ice.

Prisenberg, S., 2009. *Ice Thickness Measurements with a Miniature Electromagnetic Sensor Sled.* Osaka, Proceedings of the Nineteenth (2009) International Offshore and Polar Engineering Conference.

Sorsimo, A. & Heinonen, J., 2014. Modelling ice ridge punch tests with cohesive 3D discrete element method. *Manuscript submitted to Cold Regions Science and Technology for publication.*

Strub-Klein, L. & Sudom, D., 2012. A comprehensive analysis of the morphology of first-year sea ice ridges. *Cold Regions Science and Technology,* Volume 82, pp. 94-109.

Timco, G., Croasdale, K. & Wright, B., 2000. *An Overview of First-Year Sea Ice Ridges,* Ottawa: PERD/CHC.

Timco, G. W. & Weeks, W. F., 2010. A review of the engineering properties of sea ice. *Cold Regions Science and Technology,* Volume 60, pp. 107-129.